

Rotational Invariance In Light-Cone Quantization<sup>\*</sup>MATTHIAS BURKARDT,<sup>†</sup> AND ALEX LANGNAU<sup>‡</sup>*Stanford Linear Accelerator Center**Stanford University, Stanford, California 94309*

## ABSTRACT

In the study of the decay of a heavy scalar particle at rest in the Yukawa model at the one and two loop level, it is shown explicitly that naive light-cone quantization leads to a violation of rotational invariance. Noncovariant counterterms are constructed in detail to restore Lorentz covariance. An analysis of surface and zero mode contributions clarifies the origin of the problem.

Submitted To Physical Review D

---

<sup>\*</sup> Supported in part by the Department of energy under contract DE-AC03-76SF00515.

<sup>†</sup> Supported in part by a grant from Alexander von Humboldt-Stiftung.

<sup>‡</sup> Supported in part by a grant from Studienstiftung des deutschen Volkes.

# 1. Introduction

Light-cone quantization might be a very valuable tool toward a better understanding of the strong interaction. The main advantages of the formalism are the simple vacuum structure, the manifest boost invariance in the  $z$ -direction and the Hamiltonian formulation that leads to a very physical approach to field theory.

One of the major disadvantages of the formalism<sup>1</sup> (as for any Hamiltonian form of dynamics) is its non-manifest Lorentz invariance (here, rotational invariance). Being not manifestly Lorentz covariant one still expects that physical observables ( $S$ -matrix elements) exhibit the full Lorentz covariance of the underlying Lagrangian. Since the verification of Lorentz covariance of the  $S$ -matrix in a non-covariant formalism is in general rather tedious, it has become common practice to simply assume covariance of the  $S$ -matrix in naive light-cone quantization.<sup>2</sup> This paper deals with the problem of Lorentz covariance (in particular, rotational invariance) in light-cone quantization.

A powerful test of rotational invariance is given by examining the angular distribution of the decay products of a heavy scalar particle at rest, such as

$$\sigma \rightarrow f\bar{f}. \tag{1.1}$$

Starting out with the light-cone quantized Yukawa model<sup>3</sup>

$$\mathcal{L} = \bar{f}(i\cancel{\partial} - m)f + \phi(\square + \lambda^2)\phi + \gamma\bar{f}f\phi, \tag{1.2}$$

we note that any deviation from a uniform  $f\bar{f}$  distribution in physical  $S$ -matrix elements would indicate a serious violation of rotational invariance.

This paper investigates the decay (1.1) at the one and two loop level. A discussion beyond one loop is important in order to decide whether self-induced inertia terms,<sup>4</sup> which naturally arise from normal ordering of the Hamiltonian, could cure the problem. Violations at higher loops would mean, in particular, that any clever arrangement of self-induced inertia terms cannot restore a covariant answer for physical S-matrix elements, since self-induced inertias are of second order in the coupling.

We demonstrate an alternative treatment by adding counterterms to the Lagrangian respecting only those symmetries, which are manifestly preserved on the light-cone, i.e., transverse rotations and boosts along the  $z$ -axis. The goal of this paper is to construct them explicitly and show how rotational invariance can be restored for physical  $S$ -matrix elements. To complete the discussion, in Section 4 we address the question of why light-cone quantization leads to incorrect results, if naively applied.

## 2. Breakdown of Covariance at the One Loop Level and addition of Noncovariant Counterterms

We begin our considerations with the decay of a scalar particle into a fermion antifermion pair  $\sigma \rightarrow f\bar{f}$  at tree level. The corresponding matrix element squared is (see Fig.1)

$$\sum_{s_f, s_{\bar{f}}} |M|^2 = \text{Tr} ((\not{p}_f + m_v)(-\not{q} + m_v)) . \quad (2.1)$$

Overall light-cone energy conservation constrains the external momenta, leading to

$$\lambda^2 = \frac{m^2 + q_{\perp}^2}{q^+(1 - q^+)} . \quad (2.2)$$

Note that, in order to allow for noncovariant counterterms, two different masses have been introduced.<sup>5</sup> A vertex mass  $m_v$ , appears in the numerator, and a kinetic mass  $m$ , appears in  $P^-$  conservation and in all denominators associated with the diagram.<sup>6</sup> Eqs. (2.1) and (2.2) lead immediately to

$$\sum_{S_f, S_{\bar{f}}} |M|^2 = -2 \frac{m_v^2 - m^2}{q^+(1 - q^+)} - 2\lambda^2 + 8m_v^2. \quad (2.3)$$

Obviously rotational invariance is obtained if and only if  $m_v = m$ , *i.e.* no problems arise in tree-level physics.

At the one loop level the set of diagrams in Fig.2 contributes to the decay. Note that to order  $\gamma^4$  only interference terms between one-loop and tree level diagrams contribute. As an example we calculate the contribution from interference between a boson-exchange graph and the tree graph (see Fig.3)<sup>7</sup>

$$I_{Bos-Ex} = \gamma^4 \int_0^1 \frac{dk^+}{(16\pi^3)} d^{2(1-\epsilon)}k_{\perp} \frac{\theta(1 - q^+ - k^+)}{(q^+ + k^+)(1 - q^+ - k^+)k^+}$$

$$\frac{\text{Tr}((\not{p} - \not{k} + m)(\not{p}_2 + m)(-\not{p}_1 + m)(-\not{k} + m))}{\left(p^- - \frac{m^2 + (q_{\perp} + k_{\perp})^2}{q^+ + k^+} - \frac{m^2 + (q_{\perp} + k_{\perp})^2}{1 - q^+ - k^+}\right) \left(p^- - \frac{m^2 + (q_{\perp} + k_{\perp})^2}{1 - q^+ - k^+} - \frac{\lambda^2 + k_{\perp}^2}{k^+} - \frac{m^2 + q_{\perp}^2}{1 - q^+}\right)} \quad (2.4).$$

Using the Brodsky trick<sup>8</sup> to include instantaneous fermion contributions, performing the trace, combining energy denominators and integrating over  $k_{\perp}$ , we obtain

$$I_{Bos.-Ex.} = \gamma^4 \int_0^1 \frac{dk^+}{16\pi^3} \frac{\theta(1 - q^+ - k^+)}{(q^+ - k^+)(p^+ - q^+ - k^+)k^+} \int_0^1 d\alpha \frac{1}{\mu^2}$$

$$\left( \frac{A + B}{2} \frac{\Gamma(\epsilon)}{(M^2)^\epsilon} + \frac{C}{M^2} \right) \quad (2.5)$$

where

$$\begin{aligned}
\mu &= - \left( \frac{\alpha}{(k^+ + q^+)(1 - q^+ - k^+)} + \frac{(1 - \alpha)(1 - q^+)}{k^+(1 - q^+ - k^+)} \right) \\
M^2 &= \mu^{-1} \cdot \left( -q_{\perp}^2 \mu^{-1} \left( \frac{\alpha}{(q^+ + k^+)(1 - q^+ - k^+)} + \frac{(1 - \alpha)}{(1 - q^+ - k^+)} \right) \right. \\
&\quad \left. + \alpha \left( q^- - \frac{m^2 + q_{\perp}^2}{q^+ - k^+} - \frac{m^2 + q_{\perp}^2}{1 - q^+ - k^+} \right) + (1 - \alpha) \left( p^- - \frac{m^2 + q_{\perp}^2}{q^+ - k^+} - \frac{\lambda^2}{k^+} - \frac{m^2 + q_{\perp}^2}{q - q^+} \right) \right) \\
A &= \frac{2(4m^2q^{+2} - m^2 - q_{\perp}^2)}{(q^+ + k^+ - 1)q^+} \\
B &= -\frac{2(4m^2q^{+2} - 4m^2q^+ + m^2 + q_{\perp}^2)}{(1 - q^+)q^+}.
\end{aligned} \tag{2.6}$$

$C$  acquires terms from zero and linear order in the integration variable  $k_{\perp}$  of the Dirac trace. The linear terms give a contribution after shifting momenta. Since the expression is rather lengthy we do not display it here.

Similar steps must be performed for all the other diagrams of Fig.2. This involves renormalizing the diagrams using minimal subtraction and performing the integral over  $k^+$  and  $\alpha$  numerically. Then rotational invariance can be checked for the total one loop  $S$ -matrix element by computing the diagrams for two different sets of external momenta:

$$\begin{aligned}
\text{Set (I): } & q^+ = \frac{1}{2}, q^x = \frac{1}{4}, q^y = 0 \\
\text{Set (II): } & q^+ = \frac{1}{4}, q^x = 0, q^y = 0
\end{aligned} \tag{2.7}$$

In both cases, we have chosen  $\lambda = 1$ ,  $m = \sqrt{3/16}$ . Since both sets obey Eq. (2.1) and describe a scalar at rest, *i.e.*  $P^+ = P^-$  and  $P_{\perp} = 0$ , the answer is supposed to be the same for both of them, unless rotational invariance is broken.

For the asymmetry  $r$ , i.e. the result of the numerical integration for the difference of set (I) and set(II) , in in terms of

$$a = \frac{8\pi^3}{\gamma^4} \sum_{s_f s_{\bar{f}}} |M|^2, \quad (2.8)$$

we find  $r = 0.02a$ . That means rotational invariance is broken for physical  $S$ -matrix elements at the one loop level. In Appendix A we give details of this calculation. In particular it is shown there that the piece which violates rotational invariance comes from the instantaneous contribution in the external self-energy diagrams shown in Fig.4.

In order to keep our discussion as clear as possible, we restrict the number of spacial dimensions to two in what follows. This enables us to disentangle the specific renormalization procedure on the light-cone from the ordinary ones, since the Yukawa model is superrenormalizable in  $2 + 1$  dimensions.

The remaining goal of this section is to show that the term that violates rotational invariance is of the same form as the first term in the r.h.s. of Eq. (2.3). Thus, by allowing independent renormalizations for  $m_v$  and  $m$  one can restore rotational invariance.

Using light-cone perturbation theory (LCPT) rules one finds<sup>9</sup> for the graph in Fig. 4

$$I(q^+, q_{\perp}) = \int_0^{1-q^+} \frac{dk_{\perp} dk^+}{16\pi^3} \times \frac{\text{Tr} \left( (p - \not{h} + m)(p_2 + m) \frac{1}{2} \gamma^+ (-\not{h} + m) \right)}{(1 - q^+ - k^+) k^+ (1 - q^+) \left( p^- - \frac{m^2 + q_{\perp}^2}{q^+} - \frac{\lambda^2 + k_{\perp}^2}{k^+} - \frac{m_{\perp}^2 (q_{\perp} + k_{\perp})^2}{1 - q^+ - k^+} \right)}. \quad (2.9)$$

A change of variables  $k^+ = (1 - q^+)x$ ,  $\widehat{k}_\perp = k_\perp + xq_\perp$ , combined with use of

$$(p - q)^2 = p^-(1 - q^+) - (1 - q^+) \frac{m^2 + q_\perp^2}{q^+} - q_\perp^2 = m^2 \quad (2.10)$$

and

$$\frac{\lambda^2 + k_\perp^2}{x} + \frac{m^2 + (q_\perp + k_\perp)^2}{1 - x} = \frac{\lambda^2}{x} + \frac{m^2}{1 - x} + \frac{(k_\perp + q_\perp x)^2 + xq_\perp^2(1 - x)}{x(1 - x)} \quad (2.11)$$

yields

$$= \int_0^1 \frac{d\widehat{k}_\perp dx}{(16\pi^3)} \frac{\text{Tr}(\dots)}{x(1 - x) \left( m^2 - \frac{\lambda^2}{x} - \frac{m^2}{1 - x} - \frac{\widehat{k}_\perp^2}{x(1 - x)} \right) (1 - q^+)}. \quad (2.12)$$

To write this in a more compact form, we define the  $q^+$  and  $q^\perp$  independent function

$$f(m, \lambda) = \int_0^1 \frac{d\widehat{k}_\perp dx}{(16\pi^3)} \frac{2 - x}{\left( x(1 - x)m^2 - \lambda^2(1 - x) - m^2x - \widehat{k}_\perp^2 \right)}. \quad (2.13)$$

Discarding odd terms in  $\widehat{k}_\perp$ , which do not contribute to the integral, we obtain

$$I = \int_0^1 dx \frac{d\widehat{k}_\perp}{(16\pi^3)} \frac{(2 - x)m(1 - q^+) - (2 - x)m^2q^+}{\left( x(1 - x)m^2 - \lambda^2(1 - x) - m^2x - \widehat{k}_\perp^2 \right) (1 - q^+)} \quad (2.14)$$

$$= \frac{1 - 2q^+}{1 - q^+} f(m, \lambda) = \left( 2 - \frac{1}{1 - q^+} \right) f(m, \lambda). \quad (2.15)$$

A similar calculation for the diagram that correspond to the anti fermion self-energy, yields

$$\tilde{I} = \left( 2 - \frac{1}{q^+} \right) f(m, \lambda), \quad (2.16)$$

which contains the same function  $f(m, \lambda)$ . The total answer, i.e. the sum of  $I$  and

$\tilde{I}$ , is

$$I_{\text{tot}} = \left( 4 - \frac{1}{q^+(1-q^+)} \right) f(m, \lambda). \quad (2.17)$$

This result has the remarkable feature that it contains the same  $q^+$  dependence as the term in Eq. (2.3) that violates rotational invariance. Hence the violation of rotational invariance at the one loop level can be cured by an appropriate renormalization of  $m$  and  $m_v$ , i.e. by using different bare values for  $m$  and  $m_v$  in the light-cone Hamiltonian.

### 3. Breakdown of Covariance at the Two Loop Level

In this section it is shown that violations of rotational invariance in the light-cone formulation are not restricted to the one loop level. This statement is correct even if the one loop subdivergences are treated covariantly.

In order to constrain the number of diagrams that contribute to the  $S$ -matrix, we introduce a second fermion flavor and bosons, which change isospin, into the 2+1 dimensional Yukawa model. However all couplings at fermion-boson vertices are assigned differently, so that isospin symmetry is broken. The new interaction Lagrangian is

$$\mathcal{L}_{\text{int}} = g_{pn}\bar{p}n\phi_- + g_{pp}\bar{p}p\phi_0 + g_{nn}\bar{n}n\phi_0 + h.c. \quad (3.1)$$

In this two-flavor model only the rainbow self-energy (Fig.5) and the ladder vertex correction (Fig.6) contribute at order  $g_{pp}^2 \cdot g_{pn}^4$  to the decay  $\phi_0 \rightarrow \bar{p}p$ . All other diagrams contribute with other combinations of coupling constants and must be separately covariant, if covariance is assumed for all values of the couplings.



The rainbow self-energy contribution is shown diagrammatically in Fig.5 . The third diagram restores covariance at the one loop level. Diagrams which contain  $\delta m, \delta^{(2)}m$  are one and two loop mass counterterms respectively.

As in Section 2, we consider the instantaneous contribution to the self-energy diagrams in Fig.7 separately from the rest. Table 1 shows the result of the numerical integration for both sets of momenta in (2.7). As in the one loop case, rotational invariance is violated for the instantaneous contribution to the external self-energy diagrams.

The ladder vertex contributions yield the 6 time-orderings shown in Fig.6. The result of the numerical integration is given in Table 2 .

Thus the ladder diagrams appear to be rotationally invariant by themselves, and a possible cancellation of the noncovariant terms in the self-energy diagram cannot occur. Details of this calculation are given in Appendix B.<sup>10</sup>

In the remainder of this section we want to demonstrate that the breakdown of covariance, as in the one loop case, can be cured by an appropriate renormalization of  $m_v$  and  $m$ . Since the calculation is similar to that of the one-loop case, we restrict ourselves to an illustration of this procedure.

We start out with the matrix element in Fig.8 in two loops. In Appendix C it is shown that the two loop self-energy  $I_{self}$  contains a noncovariant piece proportional to  $C\gamma^+/p^+$  (see also ref.3), where  $C$  is independent of the incoming fermion momentum.<sup>11</sup> Thus, after on-shell mass renormalization, one finds

$$I_{self} = \left( \frac{\gamma^+}{p^+} - \frac{\bar{u}\gamma^+u}{\bar{u}u p^+} \right) C \tag{3.2}$$

$$+ (\not{p} - m)f_1(p^2) + (p^2 - m^2)f_2(p^2) .$$

The instantaneous self-energy contribution of Fig.7 becomes

$$\begin{aligned}
I &= \text{Tr} \left( (-\not{k} + m) \frac{1}{2} \frac{\gamma^+}{p^+} \frac{1}{m} (\not{p} + m) \right) C \cdot \gamma^2 \\
&= 4\gamma^2 C \frac{p^+ - k^+}{p^+} = 4\gamma^2 C \frac{2p^+ - 1}{p^+} \\
&= 4\gamma^2 C \left( 2 - \frac{1}{p^+} \right),
\end{aligned} \tag{3.3}$$

where we have set  $\not{p} = m$  for the external fermion in Fig. 7, and used the following  $\gamma^+ \gamma^+ = 0$ ,  $k^+ + p^+ = 1$  and  $\bar{u} \gamma^+ u = 2p^+$ .

An analogous calculation for the diagram which corresponds to the anti fermion self-energy, yields

$$\tilde{I} = 4\gamma^2 C \left( 2 - \frac{1}{1 - p^+} \right), \tag{3.4}$$

, so that the total contribution becomes

$$I + \tilde{I} = 4\gamma^2 C \left( 4 - \frac{1}{p^+(1 - p^+)} \right). \tag{3.5}$$

Again we see that Eq.(3.5) has the same form as the piece that violates rotational invariance in Eq.(2.3), which means that rotational invariance can be restored by tuning the vertex mass and the kinetic mass differently.<sup>12</sup>

## 4. Surface and Zero Mode Contributions

In the previous sections we have discussed the breakdown of rotational invariance in light-cone quantization and described a way to cure the problem by adding noncovariant counterterms. In order to make the discussion more complete, we will investigate in this section the question of why rotational invariance is broken if light-cone quantization is applied naively. The conclusion will be that naive light-cone quantization omits important surface and zero mode contributions.

We start our discussion with the  $n + 1$  loop self-energy diagram in Fig.8 in  $d$  dimensions and covariant perturbation theory. Since the theory is based on a manifestly covariant Lagrangian, one expects for the  $n$ -loop self-energy  $I_{self}^n$  the following structure after mass renormalization

$$I_{self}^n = (\not{p} - \not{q} - m)f_1^n((p - q)^2) + [(p - q)^2 - m^2]f_2^n((p - q)^2) \quad (4.1)$$

where  $f_i^n$  must have a spectral representation

$$f_i^n(q^2) = \int_{s_0 > 0}^{\infty} ds \frac{\rho_i^n(s)}{q^2 - s + i\epsilon} \quad (4.2)$$

with no poles for  $q^2 \leq 0$ . We discuss here only the zero mode effects induced by  $f_1^n$ . For  $f_2^n$  the same considerations can be made yielding similar results.<sup>13</sup>

One finds for the  $f_1^n$  contribution to the self-energy in  $n + 1$  loops

$$I_{self}^{n+1} = \int \frac{d^D q}{(2\pi)^D} \frac{f_1^n((p - q)^2)(\not{p} - \not{q} + m)}{((p - q)^2 - m^2 + i\epsilon)(q^2 - \lambda^2 + i\epsilon)} \quad (4.3).$$

Since problems are expected for the  $\gamma^+$ -component only<sup>3</sup>, we compute

$$\begin{aligned} \frac{1}{D} \text{Tr}(\gamma^- I_{\text{self}}^{n+1}) &= \int \frac{d^D q}{(2\pi)^D} \left( p^- - \frac{q_{\perp}^2 + \lambda^2}{q^+} \right) \frac{f_1^n((p-q)^2)}{((p-q)^2 - m^2 + i\epsilon) (q^2 - \lambda^2 + i\epsilon)} \\ &+ \int \frac{d^D q}{(2\pi)^D} \frac{1}{q^+} \frac{f_1^n((p-q)^2)}{(p-q)^2 - m^2 + i\epsilon} \end{aligned} \quad (4.4)$$

where

$$q^- = \frac{1}{q^+} (q^2 - \lambda^2 + (q_{\perp}^2 + \lambda^2)) \quad (4.5)$$

was used.

It should be emphasized that even though light-cone variables have been introduced, only algebraical steps have been performed so far, *i.e.* no breakdown of covariance can have occurred at this point. The trouble occurs when the integration over  $q^-$  is performed, in order to obtain LCPT<sub>h</sub>.

The first integral in Eq. (4.4) poses problems at the one loop level, *i.e.*  $f \equiv 1$ , when trying to perform the  $q^-$  integration. This is because the integrand falls off no faster than  $1/q^-$  for  $p^+ - q^+ = 0$  or  $q^+ = 0$ . Whereas the first case should give rise to a contribution of measure 0, we expect nonvanishing contributions from the surface term in the second case, since the denominators are multiplied by a function which diverges for  $q^+ \rightarrow 0$ .

What we encounter here is nothing else but the one loop problem of the self-energy which has been noticed by many authors.<sup>14,15,16</sup>

However, in higher loops we expect no trouble arising from this term. To illustrate this we use the spectral decomposition of Eq. (4.2) and write the first

contribution to Eq. (4.4) as

$$I_1 = \int_{s_0}^{\infty} ds \int \frac{d^D q}{(2\pi)^D} \left( p^- - \frac{q_{\perp}^2 + \lambda^2}{q^+} \right) \frac{\rho_1(s)}{((p-q)^2 - s + i\epsilon)((p-q)^2 - m^2 + i\epsilon)} \times \frac{1}{(q^2 - \lambda^2 + i\epsilon)}. \quad (4.6)$$

If sufficiently regular behavior for  $\rho_1(s)$  is assumed, the integrand falls off like  $\sim (1/q^-)^2$  or faster, which means that surface terms do not contribute.<sup>17,19</sup>

The situation is different for the second integral in Eq. (4.4) however. Performing the  $q^-$  integration leads to<sup>20</sup>

$$\frac{1}{2} \int dq^- d^{D-2} q_{\perp} \frac{1}{q^+} \frac{f_1^n((p-q)^2)}{(p-q)^2 - m^2 + i\epsilon} = \frac{1}{p^+} \delta(p^+ - q^+) \int \frac{d^D q f_1^n((p-q)^2)}{(q-p)^2 + m^2 + i\epsilon}. \quad (4.7)$$

This is because for  $p^+ \neq q^+$  the contour of the left-hand side can be chosen such that its contribution vanishes. The rest follows from

$$\frac{1}{2} \int_0^1 dq^+ \int dq^- d^{D-2} q_{\perp} \frac{1}{q^+} \frac{f_1^n((p-q)^2)}{(p-q)^2 - m^2 + i\epsilon} = \frac{1}{p^+} \int \frac{d^D p f_1^n((p-q)^2)}{(q-p)^2 - m^2 + i\epsilon}. \quad (4.8)$$

The point is that naive light-cone quantization omits the zero-mode contribution on the right-hand side of Eq. (4.7) and thereby causes a violation of rotational invariance. This also predicts that the piece that violates rotational invariance is always proportional to  $1/p^+$ , which is in perfect agreement with all our experiences at the one, two and three-loop level.<sup>16</sup> Since the right hand side of Eq. (4.7) does not depend on the outer boson mass, we see that using a heavy Pauli-Villars boson regulator instead of dimensional regularization would have taken care of the problem.<sup>21</sup>

To complete this section we want to list again the properties of the diagrams in Fig.8:

- It is very likely that non-covariances appear in any order of perturbation theory.
- The noncovariant piece is always  $p_{\perp}$  and  $p^{-}$  independent and of the form  $c \frac{\gamma^{+}}{p^{+}}$ .
- The noncovariant zero-mode contribution is independent of the outer boson mass, which explains why a Pauli-Villars regulator plays an extraordinary role among regulators.
- Dimensional regularization is not sufficient, neither is the so-called “covariant cut-off”<sup>22</sup>.
- Even supersymmetric theories suffer from this problem (see Appendix D).

## 5. Summary and Conclusions

We have shown that naive light-cone quantization leads to a violation of rotational invariance in physical  $S$ -matrix elements. To do this we investigated the decay of a heavy scalar particle at rest and observed a deviation from a uniform distribution of its decay products. The analysis shows that the effect is not restricted to one loop. Following the general arguments of Section 4 one expects a violation at any order in perturbation theory.

At the one and two loop level, we explicitly show that the problem can be cured by tuning the vertex mass  $m_v$  differently from the kinetic mass  $m$ . This procedure corresponds to adding noncovariant counterterms, which preserve only the kinematic light-cone symmetries. That requires an additional renormalization condition, compared to a manifestly covariant theory.

We suggest the decay of a heavy boson at rest because violation of covariance is obvious in this case. Once the additional counterterm is fixed the statement of renormalizability requires that *all* processes can be evaluated to the same order in perturbation theory<sup>23</sup> without encountering any further violations.<sup>24</sup> To complete our discussion, we investigated the question of why light-cone quantization goes wrong if it is not applied carefully enough. We found that nonvanishing surface contributions accompanied by a zero mode problem at one loop and missing zero mode contributions at higher loop orders cause a breakdown of the covariant structure of the theory. At this point it should be mentioned that the same problems are expected to occur in gauge theories (in  $A^+ = 0$  or any other gauge), quantized on the light-cone. As far as practical methods are concerned, such as DLCQ<sup>25</sup> or the Tamm-Dancoff-procedure,<sup>4</sup> additional violations of rotational invariance are anticipated. This is because one is forced to work with a finite value of a cut-off which by itself breaks Lorentz invariance. In this paper, we have discussed only those violations of rotational invariance which survive the continuum limit.

## Acknowledgements

One of us (A.L.) is very grateful to John Hiller for many constructive comments on the paper. We like to thank S.J. Brodsky, Hung Lu, G.Mc Cartor and B. Warr, for helpful discussions. One of us (A.L.) would like to thank Lisa Craig for bringing attention to interesting ideas which had inspiring impact on the main topic of this paper.



## APPENDIX A

Using LCPT theory for the self-energy contribution  $I_{self}$  (Fig.9), one finds

$$\begin{aligned}
 I_{self} &= \frac{\gamma^4}{16\pi^3} \int dk^+ d^{2(1-\epsilon)} k_\perp \frac{\Theta(1 - q^+ - k^+)}{(1 - q^+)k^+(1 - q^+ - k^+)} \\
 &\times \frac{\text{Tr}((p_2 + m)(p_1 + m)(p_2 + m)(-p_1 + m))}{\left(p^- - \frac{m^2 + q_\perp^2}{1 - q^+} - \frac{m^2 + q_\perp^2}{q^+}\right) \left(p^- - \frac{m^2 + (q_\perp + k_\perp)^2}{(1 - q^+ - k^+)} - \frac{k_\perp^2 + \lambda^2}{k^+} - \frac{m^2 + q_\perp^2}{q^+}\right)} \quad (\text{A.1})
 \end{aligned}$$

, where  $p_\perp = 0$  and  $p^+ = 1$ . Note that an off-shell value for  $p^-$  has been assigned in order to deal with the double pole. At the end of the calculation,  $p^-$  is taken on shell. If one shifts variables to

$$\tilde{k}_\perp = k_\perp + q_\perp \frac{k^+}{1 - q^+} \quad (\text{A.2}),$$

the Dirac trace can be reduced to the simple form  $A\tilde{k}_\perp^2 + C$ , where

$$A = 2(4m^2q^+ - 3m^2 + q^{+2}\lambda^2 - 2q^+\lambda^2 + q_\perp^2 + \lambda^2)/k_1^+ \quad (\text{A.3})$$

and  $C$  contains terms of zero and linear order in the integration variable  $\tilde{k}_\perp$  of the Dirac trace. This is correct only after terms are discarded which do not contribute to the integral. The linear terms give a contribution after shifting momenta. Since the expression is rather lengthy we do not display it here. The  $\tilde{k}_\perp$  integration can be trivially performed, yielding

$$\begin{aligned}
 &= -\frac{\gamma^4}{16\pi^3} \int_0^1 dk^+ \frac{\theta(1 - q^+ - k^+)}{(1 - q^+)^2} \frac{1}{\left(p^- - \frac{m^2 + q_\perp^2}{1 - q^+} - \frac{m^2 + q_\perp^2}{q^+}\right)} \\
 &\times \left( (1 - \epsilon)A \frac{\Gamma(-1 + \epsilon)}{(M^2)^{-1 + \epsilon}} + C \frac{\Gamma(\epsilon)}{(M^2)^\epsilon} \right) \quad (\text{A.4})
 \end{aligned}$$

where

$$M^2 = -\frac{k^+(1-k^+-q^+)}{1-q^+} \left( q_{\perp}^2 \frac{k^+}{(1-q^+)(1-q^+-k^+)} + p^- - \frac{\lambda^2}{k^+} - \frac{m^2+q_{\perp}^2}{1-q^+-k^+} - \frac{m^2+q_{\perp}^2}{q^+} \right) \quad (\text{A.5})$$

$C_{eul} = 0.577\dots$  is Euler's constant. The self-energy counterterm that corresponds to the diagram in Fig.10 is evaluated in a similar fashion. As in the self-energy diagram (see Fig.9) the instantaneous contribution is included by putting

$$p_2^- = p^- - \frac{m^2+q_{\perp}^2}{q^+} \quad (\text{A.6})$$

on energy shell.  $\delta m$  is given by

$$\begin{aligned} \delta m &= \frac{1}{2m} \gamma^2 \int dk^+ d^{(1-\epsilon)}k_{\perp} \frac{1}{k^+(1-k^+)} \\ &\times \frac{\bar{u}(p_1+m)u}{\left( p^- - \frac{m^2+k_{\perp}^2}{1-k^+} - \frac{\lambda^2+k_{\perp}^2}{k^+} \right)} \end{aligned} \quad (\text{A.7})$$

with  $p_{\perp} = 0$ ,  $p^+ = 1$  for the initial fermion. Note that it does not matter whether the instantaneous contribution is included or not, since it is  $k_{\perp}$  independent and therefore gives a vanishing contribution in dimensional regularization.

Performing steps similar to those taken before one finds

$$\begin{aligned} \delta m &= -\frac{\gamma^2}{2m} \int dk^+ (1 - \epsilon \ln N^2) \left( \frac{1}{\epsilon} - C_{eul} \right) \\ &\times (-(\lambda^2 - m^2) + m^2(1 - k^+) + k^+m^2 - 2m^2) \end{aligned} \quad (\text{A.8})$$

where

$$N^2 = -k^+(1-k^+) \left( p^- - \frac{m^2}{1-k^+} - \frac{\lambda^2}{k^+} \right). \quad (\text{A.9})$$

Table 3 shows the result for the numerical integration. The result is that rotational

invariance is broken at the one loop level. Numerically we find that the violating piece arises from the instantaneous self-energy contribution.

## APPENDIX B

We start out with the two loop rainbow self-energy diagram (Fig.5). LCPTH yields

$$\begin{aligned}
I_{rainbow} = & \frac{g_{pp}^4 g_{pp}^2}{(16\pi^3)^2} \int \frac{dk_1^+ dk_2^+ dk_{1\perp} dk_{2\perp}}{p_1^+ p_2^+ p_3^+ p_4^+ k_1^+ k_2^+} \left[ \frac{1}{(P^- - \frac{m^2+p_{1\perp}^2}{p_1^+} - \frac{m^2+q_{\perp}^2}{q^+})} \right. \\
& \left. \frac{\text{Tr} \left( (p_f + m)(p_4 + m)(p_3 + m)(p_2 + m)(p_1 + m)(-\not{h} + m) \right)}{(P^- - k_1^- - \frac{m^2+p_{1\perp}^2}{p_1^+} - \frac{m^2+q_{\perp}^2}{q^+})(P^- - k_1^- - k_2^- - \frac{m^2+p_{1\perp}^2}{p_1^+} - \frac{m^2+q_{\perp}^2}{q^+})(P^- - \frac{m^2+p_{4\perp}^2}{p_4^+} - \frac{m^2+q_{\perp}^2}{q^+})} \right. \\
+ & \left. \frac{\text{Tr} \left( (p_f + m)(p_4 + m)(-\delta m)(p_2 + m)(p_1 + m)(-\not{h} + m) \right)}{(P^- - \frac{m^2+p_{1\perp}^2}{p_1^+} - \frac{m^2+q_{\perp}^2}{q^+})(P^- - k_1^- - \frac{m^2+p_{1\perp}^2}{p_1^+} - \frac{m^2+q_{\perp}^2}{q^+})(P^- - \frac{m^2+p_{4\perp}^2}{p_4^+} - \frac{m^2+q_{\perp}^2}{q^+})} \right. \\
& \left. p_3^+ \right] \\
- & \frac{g_{pp}^4 g_{pp}^2}{(16\pi^3)^2} \int \frac{dk_1^+ dk_2^+ dk_{1\perp} dk_2^{\perp}}{p_1^+ p_2^+ p_3^+ p_4^+ k_1^+ k_2^+} \left[ \frac{1}{(P^- - \frac{m^2+p_{1\perp}^2}{p_1^+} - \frac{m^2+q_{\perp}^2}{q^+})} \right. \\
& \left. \frac{\text{Tr} \left( (p_f + m)(-\not{h} + m) \right) \text{Tr} \left( \not{h}_A + m \right) \not{h}_B + m \right) \not{h}_C + m)}{(P_{M,1}^- - k_1^- - \frac{m^2+p_{1\perp}^2}{p_1^+} - \frac{m^2+q_{\perp}^2}{q^+})(P_{M,1}^- - k_1^- - k_2^- - \frac{m^2+p_{1\perp}^2}{p_1^+} - \frac{m^2+q_{\perp}^2}{q^+})(P_{M,1}^- - \frac{m^2+p_{4\perp}^2}{p_4^+} - \frac{m^2+q_{\perp}^2}{q^+})} \right. \\
& \left. \frac{\text{Tr} \left( (p_f + m)(-\not{h} + m) \right) \text{Tr} \left( \not{h}_A + m \right) (-\delta m) \not{h}_B + m)}{(P^- - \frac{m^2+p_{1\perp}^2}{p_1^+} - \frac{m^2+q_{\perp}^2}{q^+})(P_{M,1}^- - k_1^- - \frac{m^2+p_{1\perp}^2}{p_1^+} - \frac{m^2+q_{\perp}^2}{q^+})(P_{M,1}^- - \frac{m^2+p_{4\perp}^2}{p_4^+} - \frac{m^2+q_{\perp}^2}{q^+})} \right. \\
& \left. p_3^+ \right]
\end{aligned} \tag{B.1}$$

The momenta are given by

$$p_1 = (1 - q^+, \lambda^2 - \frac{m^2+q_{\perp}^2}{q^+}, -q_{\perp}),$$

$$p_2 = p_4 = (1 - q^+ - k_1^+, \lambda^2 - \frac{m^2+q_{\perp}^2}{q^+} - k_1^-, -q_{\perp} - k_{1\perp}),$$

$p_3 = (1 - q^+ - k_1^+ - k_2^+, \frac{p_2^-}{p_2^+} p_3^+, -q_\perp - k_{1\perp} - k_{2\perp})$   
 $\tilde{p}_2 = \tilde{p}_4 = (1 - q^+ - k_1^+, \lambda^2 - k_1^-, -q_\perp - k_{1\perp}),$   
 $\tilde{p}_3 = (1 - q^+ - k_1^+ - k_2^+, \frac{\tilde{p}_2^-}{p_2^+} p_3^+, -q_\perp - k_{1\perp} - k_{2\perp})$  and  $k_1^- = \frac{k_{1,\perp}^2 + \lambda^2}{k_1^+}, k_2^- = \frac{k_{2,\perp}^2 + \lambda^2}{k_2^+},$   
 $P_{M,1}^- = \frac{p_{1,\perp}^2 + \lambda^2}{p_1^+}, P^- = \lambda^2.$  Note that the third diagram of Fig.5 which restores covariance at the one loop level can be taken into account by setting  $p_3^- = \frac{p_2^-}{p_2^+} p_3^+$  and  $\tilde{p}_3^- = \frac{\tilde{p}_2^-}{p_2^+} p_3^+.$  This rule relates the bad component of the self-energy ( $\gamma^+ p_1^-$ ) to the good component ( $\gamma^- p_1^+$ ) and covariance is achieved by construction.<sup>26</sup>

The one loop mass correction  $\delta m$  is given by

$$\delta m = \frac{e^2}{16\pi^3} \int_0^1 dk_2^+ dk_{2\perp} \frac{(1 - k_2^+)m^2 + m^2}{(-k_{2\perp}^2 + k_2^+(1 - k_2^+)(m^2 - \frac{m^2}{1 - k_2^+} - \frac{\lambda^2}{k_2^+})}.$$

The last two terms of Eq.(B.1) correspond to the two loop mass correction  $\delta^{(2)}m.$  Note that they are defined quasi-local, i.e. the  $\delta^{(2)}m$ -subtraction occurs already at the integrands before integration. This makes the expression suitable for numerical integration.

The instantaneous self-energy contribution can be obtained by subtracting a similar expression like Eq. (B.1) from  $I_{rainbow},$  where  $p_1^-$  is set on mass shell. The two loop vertex correction is computed in a similar way.

## APPENDIX C

In this section we show by explicit construction that the two loop rainbow self-energy in naive LCPT<sub>h</sub> contains a noncovariant piece of the form

$$C \frac{\gamma^+}{P^+} \tag{C.1},$$

even when all subloops have been rendered covariant.  $C$  is independent of the incoming fermion momentum  $P$ . Since by assumption the 1-loop self-energy  $I_{self}^{(1)}$  (Fig.9) is covariant, one should be able to express  $I_{self}^{(1)}$  in the form (4.1),(4.2). In this particular example we find

$$\rho_1(s) = \frac{e^2}{8\pi^3} \Omega(D) \int dx (1-x)(\tau(x))^{\frac{D}{2}-1} \Theta(\tau(x))$$

$$\rho_2(s) = \frac{e^2}{8\pi^3} \Omega(D) \int dx (2-x)(\tau(x))^{\frac{D}{2}-1} \Theta(\tau(x)) \frac{m}{m^2-s} \tag{C.2}$$

where  $\tau(x) = (x(1-x)s - (m^2x + \lambda^2(1-x)))$  was introduced.  $\Omega(D)$  is the volume of the D-dimensional unit sphere. Thus in a covariant formalism the 2-loop rainbow self-energy becomes

$$I^{(2)} = \int_{-\infty}^{\infty} \frac{d^4k}{(2\pi)^D} \frac{(\rho_1(s) + (\not{p} - \not{k} + m)\rho_2(s))}{(k^2 + i\epsilon)(\not{p} - \not{k} - m + i\epsilon)} \tag{C.3}$$

Naive LCPT<sub>h</sub> replaces  $I^{(2)}$  by  $I_{lc}^{(2)}$ , where

$$I_{lc}^{(2)} = \int \frac{ds}{(16\pi^3)^2} \int \frac{dk^+ d^{D-1}k_{\perp}}{(p^+ - k^+)^2 k^+} \frac{(\rho_1(s) + (\not{p}_{\perp} + m)\rho_2(s)) (\not{p}_{\perp} + m)}{\left(p^- - \frac{(p_{\perp} - k_{\perp})^2 + m^2}{p^+ - k^+} - \frac{k_{\perp}^2 + \lambda^2}{k^+}\right) \left(p^- - \frac{(p_{\perp} - k_{\perp})^2 + s}{p^+ - k^+} - \frac{k_{\perp}^2 + \lambda^2}{k^+}\right)}$$

$$\begin{aligned}
&= \int \frac{ds}{(16\pi^3)^2} \int \frac{dk^+ d^{D-1}k_\perp}{(p^+ - k^+)^2 k^+} \left( \rho_1(s) + \not{\tilde{h}} + m \right) \rho_2(s) \not{\tilde{h}} + m \frac{(p^+ - k^+)}{s - m^2} \\
&\quad \left( \frac{1}{\left( p^- - \frac{(p_\perp - k_\perp)^2 + m^2}{p^+ - k^+} - \frac{k_\perp^2 + \lambda^2}{k^+} \right)} - \frac{1}{\left( p^- - \frac{(p_\perp - k_\perp)^2 + s}{p^+ - k^+} - \frac{k_\perp^2 + \lambda^2}{k^+} \right)} \right)
\end{aligned}$$

and  $\tilde{p}_1 = (p^+ - k^+, p^- - \frac{k_\perp^2 + \lambda^2}{k^+} - \frac{m^2 + (p_\perp - k_\perp)^2}{(p^+ - k^+)}, p_\perp - k_\perp)$ . The problem is thus reduced to finding the noncovariant piece of the one-loop self-energy. This has been done<sup>3</sup> and the answer is of the asserted form of Eq. (C.1).

## APPENDIX D

### THE TWO-LOOP SELF ENERGY IN THE SUPERSYMMETRIC WESS-ZUMINO MODEL

When dimensional regularization is used in the Yukawa model, there is no need for a one loop noncovariant counterterm if the boson and fermion masses are equal.<sup>27</sup> This observation could be of crucial importance for the light-cone quantization of supersymmetric field theories. In fact, in Ref. 28 it has been proposed to use the (finite<sup>29</sup>)  $N = 4$  supersymmetric Yang-Mills theory as a regularized extension of light-cone  $QCD_{3+1}$ .

Compared to normal theories with similar interactions, supersymmetric theories have a less singular UV-behaviour. Since part of the problem with the violation of rotational invariance is connected with the loop regularization of light-cone singularities, one might hope that SUSY theories are less troubled by noncovariant self energies. Technically, the improved UV-behaviour arises from cancellations between various diagrams related by SUSY transformations. Perhaps something similar happens with the noncovariant self-energies in light-cone quantization. As mentioned above this is indeed the case at the one-loop level if one uses dimensional regularization in the transverse coordinates. In order to find out whether such a behaviour persists in higher loops, we will investigate the two loop self-energy of a fermion in the SUSY Wess-Zumino model<sup>30</sup>

$$\begin{aligned}
 \mathcal{L} = & -\frac{1}{2}(\partial_\mu A)^2 - \frac{1}{2}(\partial_\mu B)^2 - \frac{1}{2}i\bar{\psi}\gamma^\mu\partial_\mu\psi \\
 & - \frac{1}{2}m^2A^2 - \frac{1}{2}m^2B^2 - \frac{1}{2}mi\bar{\psi}\psi \\
 & - gm A(A^2 + B^2) - \frac{1}{2}g^2(A^2 + B^2)^2 \\
 & - ig\bar{\psi}(A - \gamma_5 B)\psi,
 \end{aligned}
 \tag{D.1}$$



where  $\psi$  is a Majorana spinor and  $A$  and  $B$  are respectively a scalar and a pseudoscalar field. The (unsubtracted) one loop self-energies for bosons and fermions in this model read

$$\tilde{\Sigma}_F = \not{p}_1 f_1(p^2) \quad \tilde{\Sigma}_B = \frac{2p^2}{m} f_1(p^2) \quad (\text{D.2})$$

where

$$f_1(p^2) = c \int d^{D-2} k_\perp \int_0^1 dx \frac{1-x}{p^2 x(1-x) - m^2 - k_\perp^2 + i\epsilon} \quad (\text{D.3})$$

( $c$  is some constant). Performing an on-shell mass subtraction one finds<sup>31</sup>

$$\Sigma_F = (\not{p} - m) f_1(p^2) + (p^2 - m^2) \frac{f_2(p^2)}{m} \quad (\text{D.4})$$

$$\Sigma_B = 2 [(p^2 - m^2) f_1(p^2) + (p^2 - m^2) f_2(p^2)]$$

where

$$f_2(p^2) = m^2 \frac{f_1(p^2) - f_1(m^2)}{p^2 - m^2}. \quad (\text{D.5})$$

Inserting these one loop corrections into the one loop self-energy yields the nested (rainbow-type) contributions to the fermion self energy at  $\mathcal{O}(g^4)$ <sup>32</sup>

$$\begin{aligned} \Sigma^{1a}(p^\mu) &= \tilde{c} \int d^D k \frac{1}{k^2 - m^2 + i\epsilon} \frac{(\not{p} - \not{k}) f_1((p-k)^2)}{(p-k)^2 - m^2 + i\epsilon} \\ \Sigma^{1b}(p^\mu) &= \tilde{c} \int d^D k \frac{1}{k^2 - m^2 + i\epsilon} \frac{2(\not{p} - \not{k}) f_1(k^2)}{(p-k)^2 - m^2 + i\epsilon} \\ \Sigma^{2a}(p^\mu) &= \tilde{c} \int d^D k \frac{1}{k^2 - m^2 + i\epsilon} \frac{2(\not{p} - \not{k}) f_2((p-k)^2)}{(p-k)^2 - m^2 + i\epsilon} \\ \Sigma^{2b}(p^\mu) &= \tilde{c} \int d^D k \frac{1}{k^2 - m^2 + i\epsilon} \frac{2(\not{p} - \not{k}) f_2(k^2)}{(p-k)^2 - m^2 + i\epsilon} \end{aligned} \quad (\text{D.6})$$

where  $\tilde{c}$  is some constant.

$\Sigma^a$  and  $\Sigma^b$  correspond to insertions of  $\Sigma^{1,\text{loop}}$  into the fermion and boson line respectively.

Following Chapter 4 we substitute in the numerator of the  $\gamma^+$  component

$$\begin{aligned}\Sigma^{1a}, \Sigma^{2a} &: -k^- \mapsto -\frac{k^2 - m^2}{k^+} - \frac{k_\perp^2 + m^2}{k^+} \\ \Sigma^{1b}, \Sigma^{2b} &: p^- - k^- \mapsto \frac{(p-k)^2 - m^2}{(p^+ - k^+)} + \frac{(p_\perp - k_\perp)^2 + m^2}{(p^+ - k^+)}.\end{aligned}\tag{D.7}$$

As we have shown there naive light-cone quantization (NLCQ) simply neglects the first term thus omitting

$$\begin{aligned}\Delta\Sigma^{1a} &= -\tilde{c}\gamma^+ \int \frac{d^D k}{k^+} \frac{f_1((p-k)^2)}{(p-k)^2 - m^2} = -\frac{\tilde{c}}{p^+} \int d^D k \frac{f_1(k^2)}{k^2 - m^2} \\ \Delta\Sigma^{1b} &= 2 \frac{\tilde{c}}{p^+} \gamma^+ \int d^D k \frac{f_1(k^2)}{k^2 - m^2} \\ \Delta\Sigma^{2a} &= -2 \frac{\tilde{c}}{p^+} \gamma^+ \int d^D k \frac{f_2(k^2)}{k^2 - m^2} \\ \Delta\Sigma^{2b} &= 2 \frac{\tilde{c}}{p^+} \gamma^+ \int d^D k \frac{f_2(k^2)}{k^2 - m^2}.\end{aligned}\tag{D.8}$$

One can easily verify that the  $\Delta\Sigma$  terms arising from  $f_2$ -insertions cancel whereas this does not happen for  $f_1$ . Thus NLCQ falls short of the correct result by an amount

$$\Delta\Sigma_{\text{NLCQ}} = \frac{\tilde{c}}{p^+} \gamma^+ \int d^D k \frac{f_1(k^2)}{k^2 - m^2} \neq 0.\tag{D.9}$$

In the beginning of this appendix we raised the hope that SUSY theories are free of the zero mode problem. Unfortunately this turned out to be false as Eq. (D.9) shows. This means that if one want to use SUSY theories as a regulator for other theories one still has to preregulate them in such a way that there are no

noncovariant terms or use some other technique (*e.g.* noncovariant counterterms) to compensate for  $\Delta\Sigma$ . This might limit the practical use of SUSY regulators in light-cone quantization considerably.

## FIGURE CAPTIONS

- 1) Tree level matrix element for the decay  $\sigma \rightarrow f\bar{f}$ . The dashed line represents a heavy boson with mass  $\lambda$  at rest:  $p^+ = p^-$ ,  $p_\perp = 0$ . The sum runs over the fermion (mass  $m$ ) spin labels  $s_f, s_{\bar{f}}$ .
- 2) Fourth order contributions to  $\sigma \rightarrow f\bar{f}$ . The  $\delta m$  insertion represents the one loop mass counterterm.
- 3) Typical contribution to the vertex correction of  $\sigma \rightarrow f\bar{f}$ .
- 4) Instantaneous contributions to the external self-energy.
- 5) Two loop rainbow self-energy contribution to  $\sigma \rightarrow f\bar{f}$ .  $\delta m, \delta^{(2)}m$  denotes the one and two loop self-energy mass correction respectively.  $I$  corresponds to a counterterm which restores rotational invariance at the one loop level.
- 6) Two loop ladder vertex correction to  $\sigma \rightarrow f\bar{f}$ . Six timeorderings add up to the covariant answer.
- 7) Instantaneous self-energy correction in two loops. Momentum labels are assigned as indicated.
- 8)  $n + 1$  loop rainbow self-energy correction.
- 9) Self-energy diagram in one loop.
- 10) One loop mass correction to the self-energy.

## TABLE CAPTIONS

- 1: Self-energy contribution to  $\sigma \rightarrow f\bar{f}$  in two loops.  $a_2$  describes the contribution from the instantaneous diagrams (Fig.7), which violate rotational invariance.  $a_1$  is the result of the numerical integration of the residual self-energy diagrams.
- 2: Result of the numerical integration of the ladder vertex correction to  $\sigma \rightarrow f\bar{f}$  (Fig.6). A rotational invariant answer is obtained for both sets
- 3: Total one loop contribution to  $\sigma \rightarrow f\bar{f}$ .

## REFERENCES

1. P.A.M. Dirac, Rev. Mod. Phys.21,392 (1949).
2. For example only certain components of tensors are calculated while other components are constructed on the basis of general Lorentz-covariance arguments.
3. M. Burkardt, A. Langnau, SLAC-PUB-5394 (1990).
4. R. J. Perry, A. Harindranath and K. G. Wilson, Phys. Rev. Lett. 65, 2959 (1990); R. J. Perry and A. Harindranath, Light-Front Tamm-Dancoff: Yukawa 1+1; The Ohio State University preprint, to be published in Phys. Rev. D; A. Harindranath and R. J. Perry, "Lowest Order Mass Corrections in 1+1 Dimensional Yukawa Model in Light-Front Perturbation Theory," to appear in Phys. Rev. D.
5. In the Hamilton formulation the kinetic mass can be identified with the mass term, that appears in the kinetic energy term for the fermions and the vertex mass is the mass that appears in the helicity-flip fermion boson vertices.

6. In this simple example there is no energy denominator.
7. J. Collins, "Renormalization" (Cambridge University Press, Cambridge 1984), page 66.
8. S. J. Brodsky, R. Roskies and R. Suaya, Phys. Rev. D8, 4574 (1973).
9. Invited Lectures, Stellenbosch Advanced Course in Theoretical Physics (Quarks and Leptons), January, 1985.
10. In the case of the ladder diagram, rotational invariance is preserved even for the corresponding off-shell Greens function. The numbers displayed in Table 2 have been obtained by setting the fermion mass off shell and equal to the boson mass in the energy denominators. Numerical difficulties occur in the on shell case at the point  $k_{\perp} \simeq 0$ ,  $k^+ \simeq 0$  since one energy denominator approaches 0 in this case. We solved this problem by integrating the difference of set (I) and set (II) directly rather than computing the difference of the integrated values for both sets.
11. Provided all noncovariant pieces have been removed from subloops.
12. It should be noted that this calculation remains correct at higher loops, provided the noncovariant piece has again the structure like  $\gamma^+/p^+$ .
13. In principle, a cancellation between noncovariant terms from  $f_1^n$  and  $f_2^n$  is conceivable. However, in practice we have not encountered an example where this actually happens. In particular, even in SUSYWess Zumino model, such terms do not cancel, as the explicit calculation in Appendix demonstrates.
14. D. Mustaki, S. Pinsky, J. Shigemitsu and K. Wilson, "Perturbative renormalization of null-plane QED," to appear in Phys.Rev.D.
15. A. Tang, Ph.D. Thesis, SLAC-REPORT No. 351 (1990).

16. A. Langnau, Ph.D. Thesis, in preparation.
17. G.Mc.Cartor,Z.Phys. C 41,271 (1988); F.Lenz in " Hadrons and Hadronic Matter ", eds. D.Vautherin, F.Lenz and J.W.Negele, Cargese, France 1989; F.Lenz, et al in Ann.Phys.(N.Y)208,1(1991),page 1.
18. It is not clear whether the zero mode terms, which appear in (4.7), are related to those zero modes which are necessary to ensure a proper description of the vacuum structure.<sup>17</sup>
19. Again one has to be careful about  $q^+ = 0$  and  $q^+ = p^+$ . It turns out that the additional term  $1/((p-q)^2 - s + i\epsilon)$  ensures sufficiently regular behavior for  $q^+ = 0, q^- \rightarrow \infty$  such that no contribution arises from this point.
20. A similar trick has been used in T.-M. Yan,Phys.Rev. D7,1780(1973) as well as in Ref. 8
21. C.Bouchiat,P.Fayet and N.Sourlas,Lett.al Nuovo Cimeto, 9(1972));S.-J. Chang and T.-M. Yan, Phys. Rev. D7,1147(1973).
22. The so-called covariant cut-off regularizes a theory by truncating the Hilbert space with respect to a given total invariant mass<sup>15</sup>
23. Of course by order we mean order in the coupling constant.
24. If there are no elementary scalars in the theory one can compare two scattering experiments in the CM-frame, which are related by a nontrivial rotation, like e.g. the total Compton cross section in QED for incoming particles along the z-direction,in comparison to the process where the incoming particles fly along the x-direction. In 1 + 1 dimensions the breakdown of parity invariance in naive light-cone quantization is conceivable. It would be of interest to check this in a nontrivial example. However, one has to be careful in select-

ing a process which is really sensitive to parity violation because quite often C-parity or Isospin symmetry (which are manifest in light-cone quantization) guarantee parity invariance for certain amplitudes.

25. H. C. Pauli and S. J. Brodsky, Phys. Rev. D32, 1993 (1987); 2001 (1987);  
T. Eller, H.-C. Pauli and S. J. Brodsky, Phys. Rev. D35, 1493 (1987);  
K. Hornbostel, Ph.D. Thesis, SLAC REPORT No. 0333 (1989) ; M.Burkardt,  
Nucl.Phys. A504,762 (1989).
26. This method works only if the tensor structure is simple enough, so that different components of the tensor can be related easily. For the vertex correction in QED in Feynman gauge this is not the case. A more general subtraction scheme will be presented elsewhere.
27. This can be directly read off from Eq. (2.9) in Ref. 3.
28. S. J. Brodsky, invited lectures presented at the 30th Schladming Winter School in Particle Physics; Field Theory, Schladming, Austria, March 1991.
29. S. Mandelstam, Nucl. Phys. B213, 149 (1983); L. Brink, O. Lindgren and B.E.W. Nilsson, Phys. Lett. 123B, 323 (1983); M. A. Namazie, A. Salam and J. Strathdee, Phys. Rev. D28, 1481 (1983).
30. J. Wess and B. Zumino, Phys. Lett. 37B, 95 (1971).
31. It should be emphasized that bosons and fermions acquire the same value for the self-mass corrections. Thus, if we would not perform a mass renormalization but rather allow the masses to change via the one loop correction, this would not induce new noncovariant effects. Since the masses of bosons and fermions would remain equal, the one-loop cancellation of noncovariant terms still applies.



32. Of course there are more diagrams contributing to the  $\mathcal{O}(g^4)$  self energy of the fermion, like *e.g.* two overlapping loops. However, those kinds of graphs do not give rise to noncovariant self energies even in non-SUSY theories and can thus be omitted in the discussion here.

Set	$a_1$	$a_2$
(I)	$-1.58 \pm 0.01$	$0.015 \pm 0.004$
(II)	$-1.58 \pm 0.01$	$-0.135 \pm 0.002$

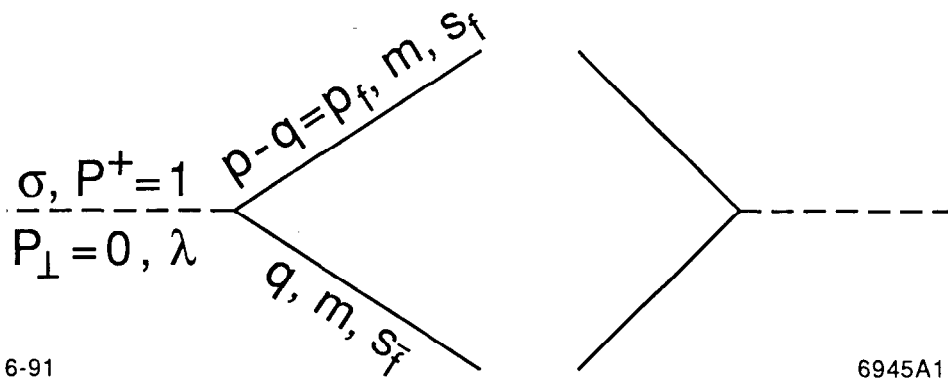
Table 1

Set	$a_1$
(I)	$-2.13 \pm 0.01$
(II)	$-2.13 \pm 0.01$

Table 2

Set	$a_1$
(I)	$0.048 \pm 0.2 * 10^{-4}$
(II)	$0.285 \pm 0.6 * 10^{-5}$

Table 3



6-91

6945A1

Fig. 1



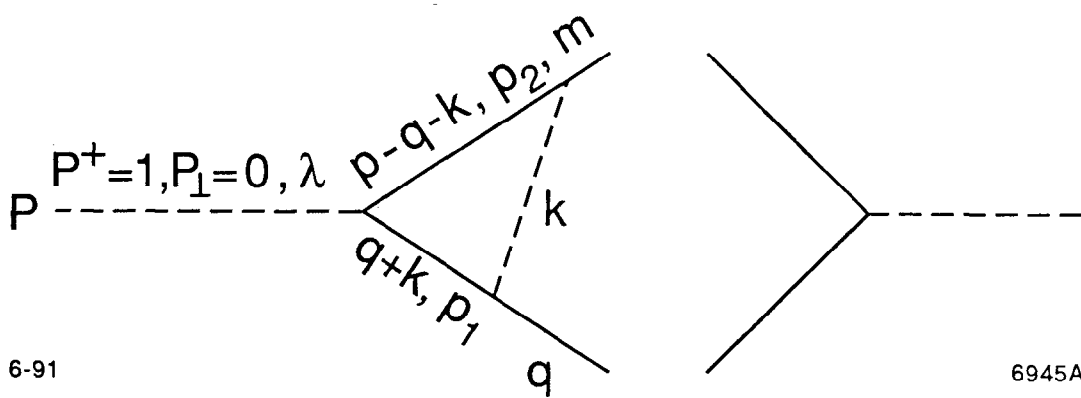


Fig. 3

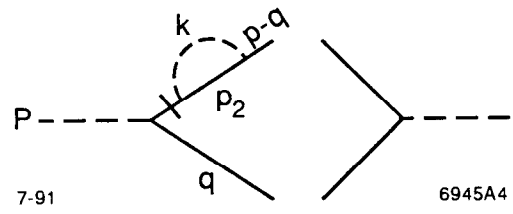


Fig. 4



$$\sum_{s_f, s_{\bar{f}}} |M|^2 = \text{[Feynman diagrams]}$$

The diagrammatic equation shows the sum of squared amplitudes  $\sum_{s_f, s_{\bar{f}}} |M|^2$  as a sum of four rows of Feynman diagrams. Each row contains two diagrams separated by a plus sign.

- Row 1:** The first diagram has a dashed line on the left and a solid line on the right, with a dashed circle around the vertex labeled  $-\delta m$ . The second diagram is similar but with a solid line on the left and a dashed line on the right, also labeled  $-\delta m$ .
- Row 2:** The first diagram has a dashed line on the left and a solid line on the right, with a dashed circle around the vertex labeled  $I$ . The second diagram has a solid line on the left and a dashed line on the right, with a dashed circle around the vertex labeled  $-\delta^{(2)}m$ .
- Row 3:** The first diagram has a dashed line on the left and a solid line on the right, with a dashed circle around the vertex. The second diagram has a solid line on the left and a dashed line on the right, with a dashed circle around the vertex labeled  $-\delta m$ .
- Row 4:** The first diagram has a dashed line on the left and a solid line on the right, with a dashed circle around the vertex labeled  $I$ . The second diagram has a solid line on the left and a dashed line on the right, with a dashed circle around the vertex labeled  $-\delta^{(2)}m$ .

The labels  $-\delta m$ ,  $I$ , and  $-\delta^{(2)}m$  are placed near the vertices of the diagrams.

6945A6

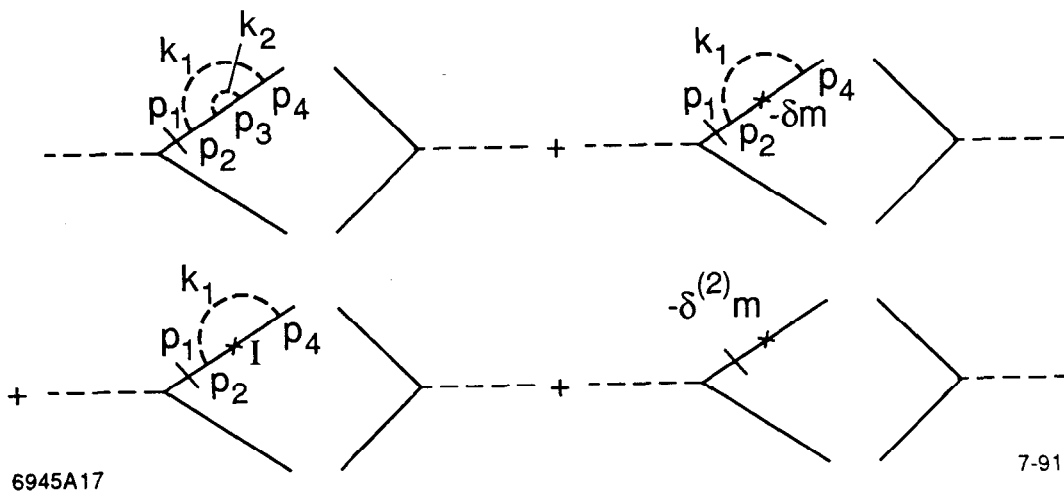
7-91

Fig. 5

$$\begin{aligned}
 \sum_{S_f, S_{\bar{f}}} |\tilde{M}|^2 = & \text{---} \langle \text{triangle} \rangle \text{---} \langle \text{triangle} \rangle \text{---} \\
 & + \text{---} \langle \text{triangle} \rangle \text{---} \langle \text{triangle} \rangle \text{---} \\
 & + \text{---} \langle \text{triangle} \rangle \text{---} \langle \text{triangle} \rangle \text{---} + \text{---} \langle \text{triangle} \rangle \text{---} \langle \text{triangle} \rangle \text{---} \\
 & + \text{---} \langle \text{triangle} \rangle \text{---} \langle \text{triangle} \rangle \text{---} + \text{---} \langle \text{triangle} \rangle \text{---} \langle \text{triangle} \rangle \text{---} + \text{C.C.}
 \end{aligned}$$

7-91 6945A10

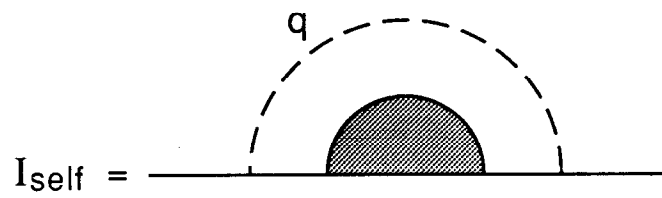
Fig. 6



6945A17

7-91

Fig. 7



6945A13

6-91

Fig. 8

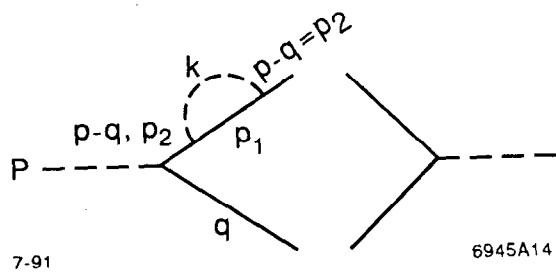
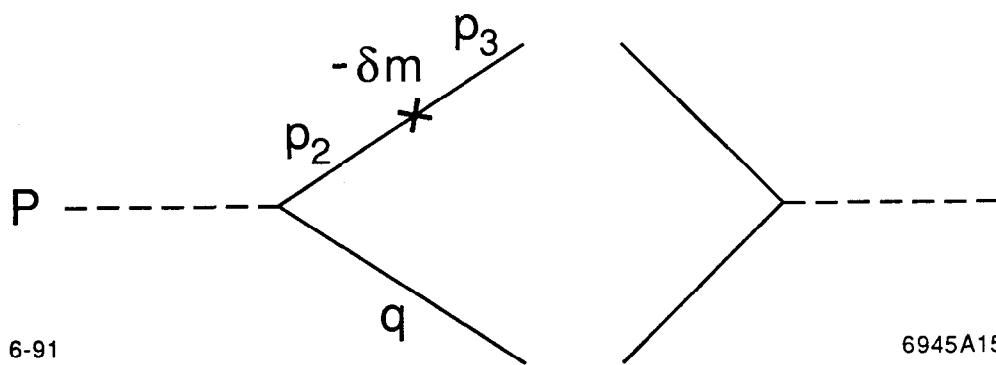


Fig. 9



6-91

6945A15

Fig. 10